Promising anti-cancer activity of batumin – a natural polyene antibiotic produced by *Pseudomonas batumici*

Maria A. Soldatkina[1], Vitalii V. Klochko[2], Svitlana D. Zagorodnya[3], Sunelle Rademan[4], Michelle H. Visagie[5], Maphuti T. Lebelo[5], Mokgadig V. Gwangwa[5], Anna M. Joubert[5], Namrita Lall[4], Oleg N. Reva[6*]

[1] Department of Molecular and Cellular Pathobiology, R.E. Kavetsky Institute of Experimental Pathology, Oncology and Radiobiology, NAS of Ukraine, Kyiv 03022, Ukraine;

[2]Dep. Antibiotics, Zabolotny Institute of Microbiology and Virology, National Academy of Science of Ukraine, Kyiv 03680, Ukraine;

[3]Dep. Viruses Reproduction, Zabolotny Institute of Microbiology and Virology, National Academy of Science of Ukraine, Kyiv 03680, Ukraine;

[4]Dep. Plant and Soil Sciences, Medicinal Plant Science Section, University of Pretoria, Pretoria 0002, South Africa;

[5]Dep. Physiology, University of Pretoria, Pretoria 0001, South Africa;

[6]Centre of Bioinformatics and Computational Biology; Dep. Biochemistry, Genetics and Microbiology; University of Pretoria, Pretoria 0002, South Africa;

*Author for correspondence: Prof. O. Reva, CBCB, Dep. Biochemistry, University of Pretoria, Lynnwood Rd, Hillcrest, Pretoria 0002, South Africa; oleg.reva@up.ac.za

Aim: To determine the computer predicted anti-cancer activity of an antibiotic batumin. **Materials & methods:** Cytotoxicity assays, cell morphology microscopy and cell cycle progression were studied in cancer and non-tumorigenic cell lines. An *in vivo* experiment on 3LL-transplanted mice was conducted to evaluate potential anti-metastatic activity of batumin. **Results & conclusions:** Cytotoxicity against melanoma and lung carcinoma cells (IC_{50} ≈ 5 μg/mL) was detected. Hypercondensed chromatin and apoptotic body formation in batumin-treated cells suggested the induction of apoptosis supported also by an observed increase in the quantity of cells occupying the sub-G1 cell cycle phase. Two-fold reduction in the number and volume of lung metastases in 3LL-bearing batumin treated mice was demonstrated. Highly specific cytotoxicity of batumin against several cancer cell lines potentiates further studies on discovery of non-toxic anticancer drugs.

Keywords: cancer; apoptosis; cell cycle; melanoma; molecular docking

Development of new anti-cancer drugs is recognized globally. According to a survey on the new anticancer drug market in Europe between 1995 and 2000 [1], new drugs had offered no substantial advantages in cancer treatment yet the cost of new drugs increased several fold. The pessimistic conclusion of this paper was negated in a subsequent publication [2], which reported increased survival of patients in the last decades due to discovery of novel anti-cancer drugs. However, all authors came to an agreement that cancer prevention procedures would be the most promising way to combat the disease in terms of cost and practical efficacy. Current measures of cancer prophylaxis are reduced to early diagnostics of cancer malformations and advertising a healthier life style. High toxicity of anti-cancer chemotherapy prevents using these medicines for cancer prophylaxis except for a reported successful application of tamoxifen for breast cancer prevention [3]. Discovery of new bioactive compounds expressing highly selective anticancer activity is of great demand for cancer treatment and prophylaxis.

It has to be admitted that the wealth of bioactive compounds discovered is not always used rationally. The number of natural and synthetic compounds is vast, but many of them are defined with a narrow activity spectrum, which was determined during the discovery of these compounds. It can be expected that several drugs may potentially have a broader use in

medicine, which has yet to be identified. Examples of unexpected therapeutic activities of various natural secondary metabolites were overviewed by Vaishnav & Demain [4], who showed a great deal of unexplored potential of previously discovered bioactive compounds. Innovative computational tools of molecular docking and pharmacophore analysis allow prediction of therapeutic activities of natural and synthesized chemical compounds [5]. These techniques may aid in discovery of new activities of known drugs.

In this paper, discovery of the promising anti-cancer activity of the antibiotic batumin is presented. This antibiotic is produced by *Pseudomonas batumici* and is known as an active anti-bacterial agent against *Staphylococcus aureus* including methicillin resistant variants of this pathogen [6, 7]. Impairment of the fatty acid biosynthesis in bacteria by inhibiting the activity of the protein enoyl-ACP reductase (FabI) was suggested as a mode of action of batumin [8]. However, computer modeling of molecular docking of batumin to FabI failed in the identification of any possible binding site for this antibiotic in the active center of FabI [9]. By contrast, a high affinity of batumin to the Rossmann fold domain of aminoacyl tRNA synthetases was predicted in this work and an alternative model of the antimicrobial action of batumin was suggested. Controversies in the proposed models were pointed out in a subsequent publication [10]. In the current study, computer based high-throughput screening was carried out against the PharmaDB database in order to address these disagreements and to identify alternative molecular targets of batumin. Surprisingly, the search did not identify any of the previously proposed molecular targets but indicated possible affinity of batumin to active centers of several cancer related proteins. Furthermore, this study demonstrated that batumin exerts cytotoxic and apoptotic activity in cancer cell lines.

Batumin is a linear polyene antibiotic encoded by a large hybrid operon of polyketide synthases and nonribosomal peptide synthetase (PKS-NRPS) comprising of 30 genes [8, 9]. Natural PKS-NRPS encoded polyene compounds are versatile in their chemical structures and biological activities [11], which include many potential and clinically approved antibacterial, antiviral, antifungal and anti-cancer drugs [12]. Detailed stereochemical analysis of kalimatacin/batumin antibiotics has recently been published [13]. Polyene antibiotics are convenient products for genetic engineering as all their structural versatility can be designed by manipulations of a limited number of functional building units [14]. Hence, knowledge of the molecular

mechanisms of action of bioactive compounds will aid in design and optimization of new antibiotics.

Materials & methods

Extraction of batumin

The antibiotic batumin was obtained from culture medium of the producer-strain *Pseudomonas batumici* UCM B-321 as previously described [15]. The producer-strain was cultivated in a 5 l fermenter Biostat M5 (Sartorius, Germany) with automated control of growth parameters in aerobic conditions at 25°C for 65 h. Extraction of batumin was carried out from acidified culture liquid by chloroform (1:2). The extract was evaporated and purified by preparative chromatography in a 20×1.5 cm column with silicagel (Fluka, USA) with a pore size of 40-100 μm in liquid phase of benzene:acetone (1:1). Batumin yield was detected by TLC using Merck plates. All active fractions were combined and vacuum dried. Presence of batumin in the resulted substance was detected by HPLC and proton magnetic resonance (PMR) previously described [15].

Cancer cell lines

The human epidermoid carcinoma (A431), human lung adenocarcinoma (A549) and an *in vitro* culture of transplantable Lewis lung carcinoma (3LL) cell lines were obtained from the Bank of Cell Lines from Human and Animal Tissues of R.E. Kavetsky Institute of Experimental Pathology, Oncology and Radiobiology, NAS of Ukraine (IEPOR, Kyiv, Ukraine). The cells were cultured *in vitro* in Dulbecco's Modified Eagles Medium (DMEM) culture medium supplemented with 10% fetal bovine serum (FBS), 100 units/mL penicillin, 100 μg/mL streptomycin sulphate and 0.25 μg/mL amphotericin B in 5% CO_2 atmosphere at 37ºC.

The A431; human cervical adenocarcinoma (HeLa) and human epithelial metastatic (pleural effusion) mammary gland breast adenocarcinoma (MCF-7) cell lines were obtained from the European Collection of Cell Cultures (ECACC, England, UK). Madin-Darby bovine kidney epithelial (MDBK) cell line was obtained from Merck. The human pigmented melanocyte metastatic (inguinal lymph node) melanoma (UCT-Mel 1) and human spontaneously transformed immortalized skin keratinocyte (HaCat) cell lines were generously donated by Prof.

Lester Davids from the Department of Human Biology at the University of Cape Town, RSA. Fetal bovine serum (FBS) and antibiotics were purchased from Separations (Pty) Ltd. (Randburg, Johannesburg, RSA). The Cell Proliferation Kit II (XTT), Bouin's solution, Hematoxylin solution Gill NO. 1, Eosin Y solution (alcoholic) and xylenes were purchased from Sigma Chemicals Co. (St. Louis, MO, USA). All other chemicals and reagents were of analytical grade and acquired from Sigma Chemicals Co. (St. Louis, MO, USA).

The MCF-7 and HeLa cell lines were maintained in Eagle's Essential Medium (EMEM). The A431, UCT-Mel 1 and HaCat cell lines were maintained in DMEM. All cell lines were supplemented with 1% antibiotics (100 µg/mL penicillin, 100 µg/mL streptomycin and 250 µg/L fungizone) and 10% heat-inactivated FBS. The cells were grown at 37°C in a humidified incubator set at 5% CO_2. Cells were sub-cultured with 0.25% (w/v) trypsin 0.53 mM ethylenediaminetetraacetic acid (EDTA) for a maximum of 15 min every 2-3 days after they had formed an 80% confluent monolayer.

***In vitro* cytotoxicity assays**

To analyze the effect of batumin on cell viability, MTT [16] and XTT [17] assays were performed. A stock solution of 10 mg/mL batumin was prepared. Serial dilutions were made to achieve target concentrations of batumin in a wide range 3.125 – 400 µg/mL assuming that the cytotoxic activity of batumin may be culture specific. Plates were then incubated for 24 h at 37ºC and 5% CO_2 to allow cells to attach to the bottom of the wells. Subsequently, cells were exposed to batumin in dimethyl sulfoxide (DMSO) 2% medium supplemented with 2.5% FBS as described below. The control wells included vehicle-treated cells exposed to 2% DMSO; cells propagated in growth medium and cells exposed to actinomycin D [18] in a range of concentrations 0.002 – 0.5 µg/mL. Actinomycin D was one of the first antibiotics that was discovered to have antiproliferative-, apoptotic- and anticancer activity and it's mechanism of action ultimately also exerts an effect on p53. As such, Actinomycin D was considered as an appropriate positive standard control in this study. For the MTT assay, cells (1×10^3 cells/well) were seeded in 100 µl in 96-well microtitre plates at a concentration of 1×10^3 cells/mL and incubated with batumin for 48 h at 37ºC in a DMEM medium supplemented with 2.5% FBS. The cells were routinely treated with 3-[4,5-dimethylthiazole-2-yl]-2,5-diphenyltetrazolium bromide

(MTT reagent) by the standard protocol. The colorimetric reaction was evaluated by means of an ELISA reader (Awareness Technology Inc, USA) at 545 nm wavelength with a reference wavelength 690 nm.

For the XTT assay, cells were seeded in 100 µl DMEM medium in 96-well microtitre plates at a concentration of 1×10^5 cells/mL. Plates were incubated with batumin for a further 72 h at 37ºC. Subsequently, 50 µl 3-[4,5-dimethylthiazole-2-yl]-2,5-diphenyltetrazolium bromide (XTT reagent) was added to a final concentration of 0.3 mg/mL and the plates were incubated for 2 h. After the incubation period, the absorbance of the color complex was read at 490 nm with a reference wavelength set at 690 nm using a BIO-TEK Power-Wave XS multi-well plate reader (A.D.P, Weltevreden Park, South Africa).

***In vivo* study**

For the *in vivo* study of anti-cancer activity of batumin, 13 two-month-old female C57BL mice weighing 20–22 g were obtained from the animal facility of IEPOR. All procedures were carried out according to the rules of the Ethic Committee of IEPOR and were approved by the Ethic Board of IEPOR.

Lewis lung carcinoma (3LL) cells were cultured *in vitro* in 50 mLl flasks with DMEM culture medium supplemented with 10% FBS, 100 units/mL penicillin, 100 µg/mL streptomycin sulphate in 5% CO_2 atmosphere at 37ºC. When the cells reached confluence, they were routinely detached with 0.5% trypsin solution, washed with phosphate buffer saline (PBS), counted in a hemocytometer and used for transplantation to experimental animals.

3LL cells (1×10^6 cells / 100 µL PBS per animal) were transplanted by intra-muscular (i.m.) injections in the right hind legs of mice. After transplantation, the animals were randomly distributed into 2 groups: 7 animals of the control group were treated with intraperitoneal (i.p.) injections of 0.5 mL of the physiologic solution and 6 animals of the experimental group were treated with i.p. injections of 0.35 mg batumin in 0.5 mL of physiologic solution per animal. Physiological solution and batumin were injected at days 2, 4, 7, 9, 11, 14, 16, 18, 21 following the 3LL transplantation. Dosage of batumin was estimated from earlier reported data on the minimal toxic dose (MTD) of 150 mg/kg of batumin per mouse (Kiprianova EA, personal

communication). This level of toxicity was confirmed in the current study using the MTT cytotoxicity assay with MDBK bovine kidney cells (Merck) by treating the cells with 100, 25, 17, 10, 5, 2.5 and 1.25 μg/mL batumin. The estimated IC50 on the MDBK was 35.3 μg/mL.

Tumor growth dynamics was monitored daily by means of calipers starting from day 7 after the tumor cell transplantation when the tumors became palpable until the end of the experiment at day 23 after the transplantation. On the last day of the experiment, animals were sacrificed by narcosis. Primary tumors were removed and weighed. The number of lung metastases and their volume were routinely analyzed using a binocular microscope and millimeter scale.

Assessment of the antitumor and anti-metastatic activities of batumin was performed at the day 23 after the tumor transplantation. Primary tumor volume was calculated by the equation:

$$V = \frac{\pi(D_1 \times D_2 \times D_3)}{6}$$

where D_1, D_2 and D_3 are the longitudinal, lateral and sagittal lengths of the tumor.

The volume of metastases was estimated by the following equation [19]:

$$V = \sum\left(n_i \times \frac{\pi \times d_i^3}{6}\right)$$

where n_i is the number of metastases with average diameters d_i of 0.5 mm, 1.0 mm, 1.5 mm and greater with a step of 0.5 mm.

Cell morphology

Exponentially growing cells were seeded at 2×10^5 cells per well in 6-well plates on heat-sterilized coverslips. After 24 h of incubation at 37ºC and 5% CO_2 to allow for cell adherence, cells were exposed to a range of concentrations (4.5, 9 and 12 μg/mL) of batumin. Cells propagated in growth medium and vehicle-treated (1% DMSO) cells were included as controls. Subsequently, cells were incubated at 37°C for a period of 72 h. Following the incubation period, the media was discarded and the cells were washed with PBS. The cells were stained with the

standard hematoxylin and eosin staining procedure as previously described [20]. Microscopy slides were prepared and the cells were observed under a light microscope (ZEISS, Primovert) at 40X magnification.

Cell cycle progression

Flow cytometry and propidium iodide were utilized to investigate the DNA content in order to determine the influence of batumin on the cell cycle progression and possible apoptosis induction. Propidium iodide stains the DNA and thus enables the quantification of DNA correlating with stages of the cell cycle during cell division [21]. Cells were plated at 500,000 cells per 25 cm^2 flask and left for 24 h to attach. Subsequently, cells were exposed to batumin for 72 h at 37°C. Cells propagated in growth medium and vehicle-treated cells were included as negative controls and cells treated with actinomycin D were included as a positive control of apoptosis induction. After exposure to batumin, cells were trypsinized in 0.25% (w/v) trypsin with 0.53mM EDTA for approximately 15 min or till cells are rounded and ready to detach from the flask surface. Then 10^6 cells were centrifuged for 5 min at 300 x *g*. The pellet was resuspended twice in ice-cold PBS. The supernatant was discarded and cells were resuspended in 200 µl of ice-cold PBS containing 0.1% FBS. Ice-cold 70% ethanol (4 mL) was added in a drop-wise manner and cells were stored at 4ºC for 24 h. Cells were pelleted by centrifugation for 5 min. The supernatant was removed and cells were resuspended in 1 mL of PBS containing propidium iodide (40 µg/mL), 0.1% triton X-100 and RNase A (100 µg/mL), and incubated at 37ºC in 5% CO_2 for 45 min. Cells were analysed by means of a FC500 flow cytometer Beckman Coulter (Brea, CA, USA). Data from cell debris (particles smaller than apoptotic bodies) and clumps of 2 or more cells were removed from further analysis. Cell cycle distributions were calculated by Cyflogic version 1.2.1 (Pertu Therho, Turko, Finland), which assigns relative DNA content per cell to sub-G_1, G_1, S and G2/M phases.

***In silico* molecular docking**

The chemical structure of batumin has been described in previous publications [6, 8, 9]. Accelrys Discovery Studio 4.0 was used to generate a collection of 94 spatial conformations of batumin, which were then used for querying the PharmaDB database that contains more than 140,000 pharmacophore models [22]. Thereafter, the molecular docking of batumin molecules was

performed against identified target proteins by using the LibDock algorithm [23]. Electronic structures of the target proteins in PDB format with identified binding sites and chemical structures of known inhibitors were obtained from RCSB PDB database (www.rcsb.org, [24]).

Statistical analysis

Statistical analysis of the results was performed by the descriptive statistics, Student's t-test and Mann-Whitney U test, with the use of Microsoft Excel and Microcal Origin programs. All assays were performed a minimum of three times. The fifty percent inhibitory concentration (IC_{50}) of the compound was calculated using the GraphPad Prism 4 program (GraphPad Software, Inc., CA, USA). The safety margin of the compound was also taken into account by calculating the selectivity index (SI) values as a ratio of IC_{50} determined on non-cancerous cells to IC_{50} cancerous cell line. The SI value gives an indication of the specificity towards either the cancerous cell line or the non-cancerous cell line [25]. An SI value greater than one indicates a specificity towards the cancerous cell line; whereas an SI value less than one implies that the compound is more toxic towards the non-cancerous cell line. The SI value of the compound was calculated as the ratio of the IC_{50} value on a non-cancerous cell line to the IC_{50} value on a cancerous cell line.

Flow cytometry analysis involved at least 10,000 events and was repeated three times, where the mean and the standard deviation were calculated. Flow cytometry data was analyzed using Cyflogic version 1.2.1 (Perko, Finland). *P*-values less than 0.05 were regarded as statistically significant.

Results

Search through PharmaDB and molecular docking

Batumin has been previously identified as an anti-staphylococcal antibiotic [7]. However, the search through PharmaDB revealed a possible affinity of batumin to active centers of cancer related proteins p53 and Act1. Anticancer activity of batumin has never been reported before. In previous studies, it was suggested that batumin could suppress the growth of *Staphylococcus aureus* by binding to protein FabI and impairing fatty acid biosynthesis in bacteria [8]. However, another study determined by molecular docking that batumin had no affinity to FabI, but it could

bind to the Rossmann fold domain of aminoacyl tRNA synthetases similar to the antibiotic mupirocin [9]. This hypothesis was criticized in a subsequent paper [10]. This paper reported that in contrast to mupirocin, which resulted in a strong inhibition of the protein biosynthesis in *S. aureus* in 10 min after treatment, batumin suppressed mainly fatty acid biosynthesis resembling the activity of triclosan – a FabI inhibitor. Surprisingly, the search through the PharmaDB returned neither FabI, nor tRNA synthetases as possible targets of batumin which caused doubts regarding the accuracy of the pharmacophore approach of identification of possible molecular targets. Nonetheless, due to the importance of discovering new anti-cancer drugs, it was decided to continue studying the possible anti-cancer activity of batumin by molecular docking to the predicted molecular targets and by the evaluation of the cytotoxicity of batumin on cancer cell lines.

A possible affinity for batumin was predicted against the mouse double minute 2 homolog (MDM2) active center of p53, which is responsible for an inhibition of p53 apoptosis activity. Blocking this center by ligands potentially restores apoptosis in cancer cells [26]. The molecular structure of MDM2 was obtained from the RCSB PDB database [24] (accessions IDs 4QO3 and 4OQ4). X-Ray proved locations of several MDM2 inhibitors in the active center of the protein, which were provided in the database [27, 28]. The molecular structures of these inhibitors were used in this study as a positive control for the LibDock molecular docking algorithm. In total, 94 possible conformations of batumin were predicted by using the Search Small Molecule Conformations tool of the Accelrys Discovery Studio 4.0. Receptor binding sites of the target proteins were defined by locations of previously predicted inhibitors as indicated in the 4QO3 and 4OQ4 structures. LibDock algorithm for docking small molecules into an active receptor site implemented in Accelrys Discovery Studio 4.0 was used to perform the molecular docking of all 94 predicted conformations of batumin. Ligand positions were ordered by the absolute binding energy and the positions with the highest energy were analyzed. Docking of batumin against the MDM2 binding site indicated that this molecule could potentially bind to the MDM2 center of p53 with energy similar to that estimated for other known inhibitors (Table 1).

Table 1. LibDock molecular docking of batumin against the MDM2-p53 binding site in comparison to the binding energy estimated for known MDM2 inhibitors.

Chemical compounds	Estimated absolute energy of binding (kcal/mol)	LibDock scores of predicted binding affinity	RCSB Database IDs (www.rcsb.org)
Comp 3	76.2288	144.291	4OGN
Comp 46	71.7195	165.291	4OGT
Comp 47	70.9667	103.058	4ODF
Comp 25	65.2897	69.559	4OAS
Comp 4	60.7294	139.235	4ODE
Comp 49	59.4362	129.946	4OGV
Comp 48	58.9756	124.285	4OCC
Batumin	51.7425	85.6977	This experiment
tetra-substituted imidazole	51.3536	79.2149	4OQ3

A similar estimation of a binding energy of 53.1 kcal/mol was obtained by docking the batumin chemical structure against the active center of the protein Act1 (DCSB ID 4GV1, [29]).

Cytotoxicity assays

Preliminary assays for the anti-cancer activity of batumin were performed independently in two laboratories at the University of Pretoria (UP) in South Africa by XTT approach [17] and at IEPOR by MTT approach [16]. To ensure unbiasedness of results to laboratory specific conditions and cell cultures, the experiments on cytotoxicity were performed in both institutes in parallel using own protocols and cell cultures without any exchange of results until the experiments were finished. At UP, batumin was tested in several cell lines in concentrations of 3.125, 6.25, 12.5, 25, 50, 100, 200 and 400 μg/mL (Fig. 1). This rather wide range of concentrations was applied due to absence of any preliminary data on sensitivity of cancer cells

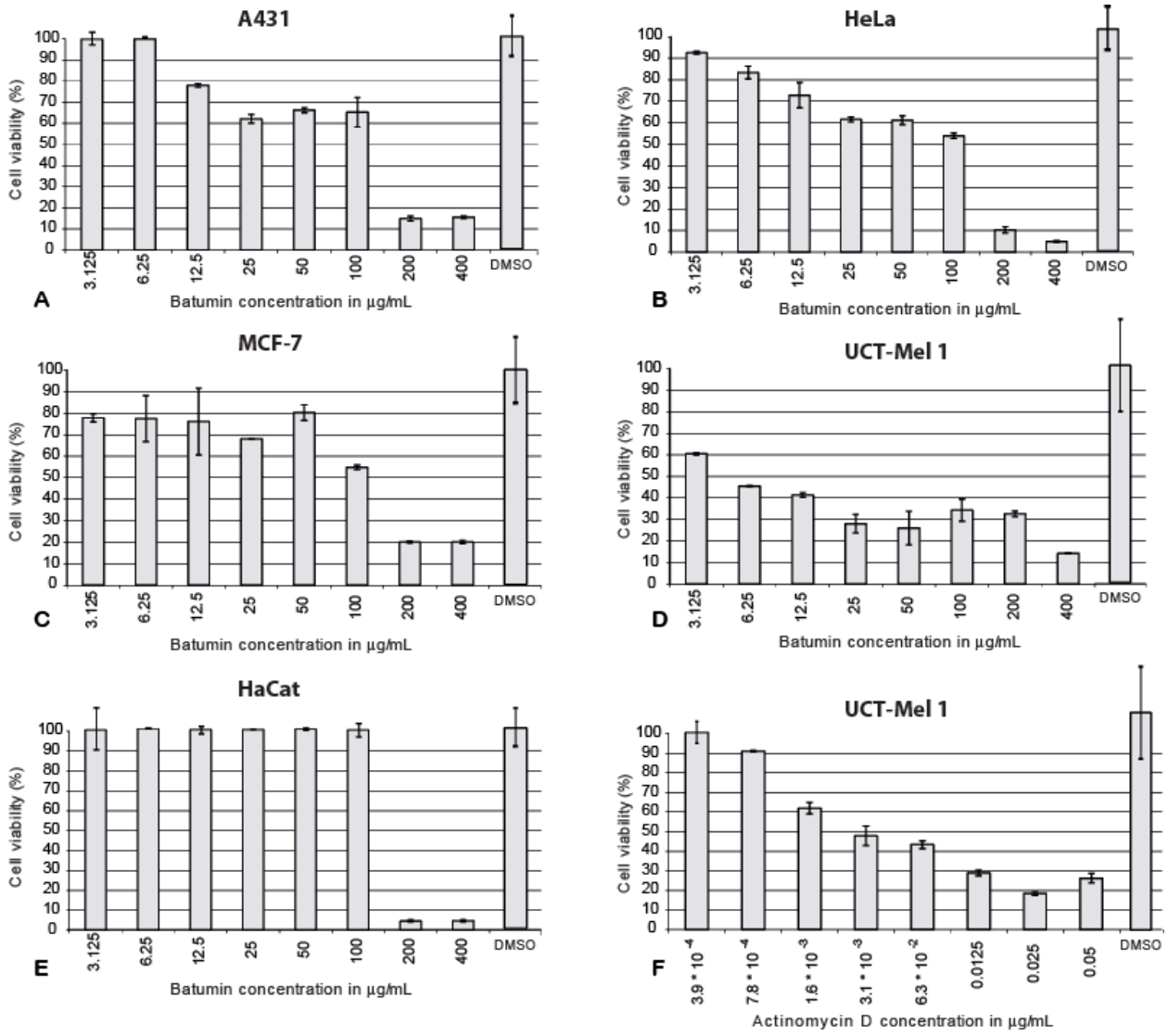

Figure 1. Dose dependent cytotoxicity effect of batumin revealed on cell cultures by XTT analysis. A431 squamous cell carcinoma (A); HeLa cervical cancer (B); MCF-7 breast cancer (C); UCT-Mel 1 melanoma (D); HaCat skin keratinocytes (E); and effect of actinomycin D on UCT-Mel 1 (F).

to batumin and because of an assumption that the toxicity of batumin may be culture specific. The dose dependent effect of batumin was observed with the highest activity against the UCT-Mel 1 melanoma cell line (IC_{50} = 4.5 µg/mL). By contrast, batumin showed no activity against the normal skin keratinocytes (HaCat) at concentrations up to 100 µg/mL. Table 2 shows IC_{50} and SI values calculated for batumin based on the cytotoxicity data in Fig. 1 in comparison to the activity of actinomycin D used in this study as a positive control. Batumin in average was 3 to 4 order of magnitude less active than actinomycin D, but in contrast to the latter antibiotic, the

activity of batumin was strongly culture specific. As it is evident from SI values, the melanoma skin cancer cell line was 20-fold more sensitive to batumin than the other cancer cell lines evaluated in this assay and the normal keratinocytes.

Table 2. Cytotoxic activity of batumin against cancer cell lines A431, MEL-1, HeLa and MCF-7; and against normal skin keratinocytes HaCat as revealed by XTT.

Cell line	**Batumin IC_{50} (μg/mL) ± SD**	**Selectivity Index (SI) of batumin**	**Actinomycin D IC_{50} (μg/mL) ± SD**	**Selectivity Index (SI) of actinomycin D**
A431 – Squamous cell carcinoma	171.3 ± 6.8	0.6	0.0074 ± 3.6	4.1
UCT-Mel 1 – Melanoma skin cancer	4.5 ± 2.7	22.5	0.0073 ± 3.7	4.1
MCF-7 – Breast cancer	140.6 ± 6.9	0.7	0.0082 ± 5.6	4.6
HeLa – Cervical cancer	128.5 ± 3.7	0.8	0.0093 ± 6.1	5.2
HaCat – Skin keratinocytes	101.4 ± 16.7	-	0.0018 ± 7.6	-

The cytotoxicity of batumin was evaluated at IEPOR in the human epidermoid carcinoma (A431) and human lung adenocarcinoma (A549) cell lines. A dose dependent effect of batumin was observed in both cancer cell lines (Fig. 2) with an IC_{50} around 20-25 μg/mL for A431 and 5-10 μg/mL for A549 cells. For experiments conducted at IEPOR, batumin was almost 8 times more toxic against A431 cells than in the experiment on the same cell line at UP. It may reflect either the different load of cancer cells used in these two laboratories – 5×10^5 for XTT at UP and 5×10^3 for MTT at IEPOR. Batumin showed almost the same strong toxicity against A549 cells in the MTT assay as against melanoma cells (UCT-Mel 1) in parallel experiments at UP (Fig. 1 and

Table 2) in the XTT assay; however, the cell load in the XTT assay was two order of magnitude higher.

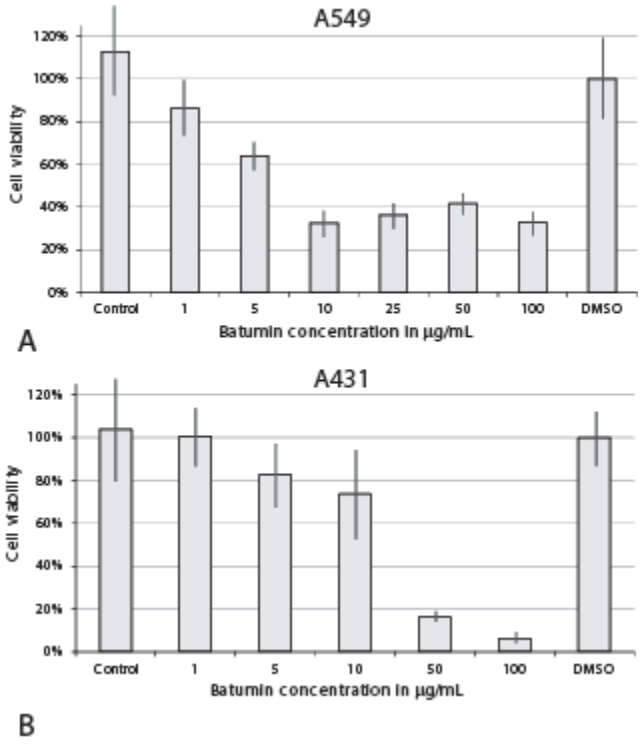

Figure 2. Dose dependent cytotoxicity effect of batumin revealed on cell cultures by MTT analysis. A431 squamous cell carcinoma (A) and A549 human lung adenocarcinoma (B) cells.

Melanoma cell morphology

Light microscopy was conducted to assess the effect of batumin on the morphology of UCT-Mel 1 melanoma cells. Generally, different types of tissues stained by haematoxylin and eosin display nuclei that are blue to purple in color, whereas the cytoplasm and extracellular matrix display varying pink color shades. Different types of cell death can be distinguished from one another by specific morphological characteristics, which include the loss of plasma membrane integrity, fragmentation of cells and nucleus into apoptotic bodies and engulfment of remaining fragments of one cell by another [30].

Batumin was tested on the UCT-Mel 1 cell line at concentrations of 3, 6 and 12 µg/mL (Fig. 3). Morphological characteristics of apoptotic cell death, such as hypercondensed chromatin and apoptotic body formation were observed at a lower concentration of batumin (Fig. 3A). Furthermore, exposure to higher concentrations of batumin (6 and 12 µg/mL) resulted in a prevalence of vesicle formation, which could be an indicative of autophagy induction (Fig. 3B-C). UCT-Mel 1 samples treated with a vehicle control (1% DMSO) had a higher cell density than the cells treated with higher concentrations of batumin. Normal cell division process was observed in the control cells that was almost absent in the treated cells (Fig. 3D).

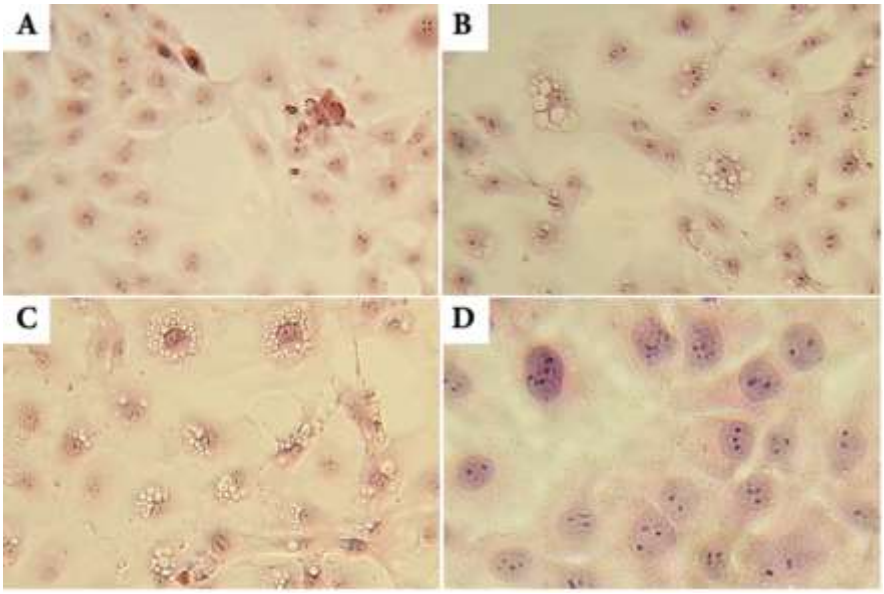

Figure 3. Hematoxylin and eosin staining of UCT-Mel 1 cells under different treatment regiments. Cells treated by 4.5 µg/mL (A); 9 µg/mL (B); and 12 µg/mL (C) of batumin, and 1% DMSO control (D) after 72 h under 40X magnification.

Table 3. Effect of batumin injections on the volume of tumors and number of metastases in experimental mice compared to the control group of mice.

Experiment	**Primary tumour volume**	**Metastatic volume**	**Number of metastases**
Control group	2.562 ± 0.563 cm^3	19.58 ± 5.72 cm^3	21.43 ± 5.42
Experimental group	2.19 ± 0.197 cm^3	7.53 ± 5.43 cm^3	11.57 ± 3.23

Cell cycle progression

The effect of batumin on cell cycle progression was investigated by means of flow cytometry. Exposure to batumin induced a statistically significant increase in the quantity of cells occupying the sub-G_1 phase suggesting induction of apoptosis (Fig. 4 and Table 4). Exposure to batumin resulted in a statistically significant increase in the number of HaCat cells occupying the sub-G_1 phase to 14% when compared to the vehicle-treated cells (3%). Furthermore, possible apoptosis induction was more prominent in the UCT-Mel 1 cells with the number of cells occupying the sub-G_1 phase being significantly increased up to 39% when compared to the vehicle-treated cells (3%). Batumin exposure also resulted in a statistically significant decrease in the number of HaCat cells present in the S phase (9%) and in the G_2/M phase (18%) when compared to the vehicle-treated cells. Treatment of UCT-Mel 1 cells with batumin decreased the percentage of cells in the G_1 phase to 51% compared to 80% in vehicle-treated cells. Similarly, only 8% of the treated cells were in the G_2/M phase compared to 14% in the vehicle-treated cells.

Table 4 Percentage of cells in different cell cycle phases determined by cytometry with Cyflogic 1.2.1 (Perttu Terho & Cyflo Ltd).

Cell lines	Sub-G_1 phase	G_1 phase	S phase	G_2/M phase
HaCat				
Vehicle-treated cells	2.93±1.66	61.01±2.07	13.68±1.63	22.37±1.22
Batumin-treated cells	14.14±1.32*	58.80±1.55	8.87±1.54*	18.2±1.31*
UCT-MEL 1				
Vehicle-treated cells	2.73±0.65	80.07±1.8	3.05±0.75	14.14±2.13
Batumin-treated cells	38.66±2.21*	51.22±0.99*	2.59±0.7	7.53±1.94*

*Statistically reliable difference ($P \leq 0.05$) in numbers of cells present in the given cell cycle phase in the batumin treated cells compared to the vehicle-treated cells.

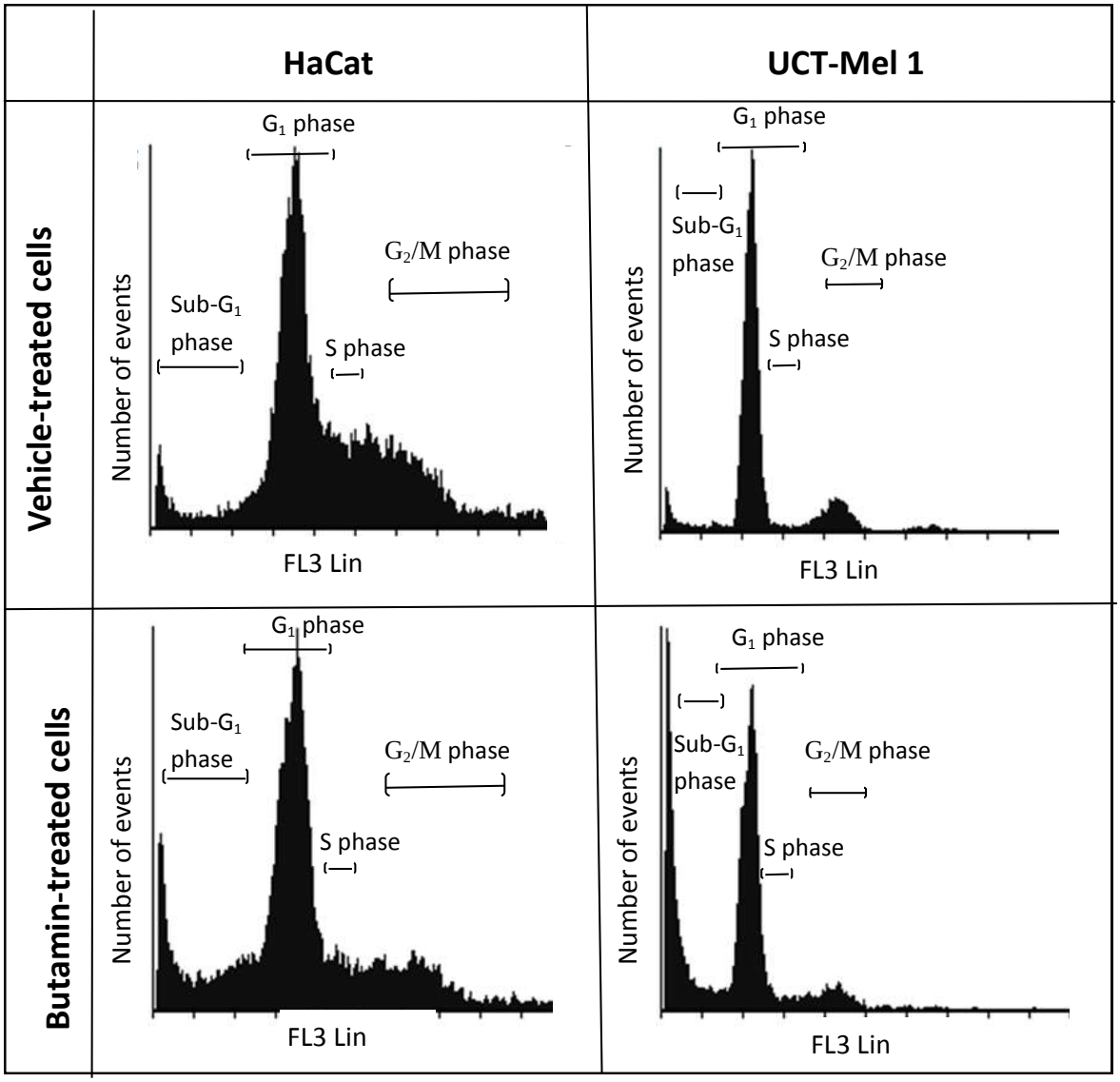

Figure 4. Occupation of cell cycle phases by cells of HaCat and UCT-Mel 1 in control and after batumin treatment. Histograms represent the distribution of batumin and vehicle treated cells in different cell cycle phases. Exposure to batumin caused an increase in the number of cells occupying the sub-G_1 phase with a corresponding decrease in all other cell phases in both cell lines. This effect was stronger on melanoma UCT-Mel 1 cells compared to HaCat normal skin keratinocytes.

Anti-metastatic activity of batumin

The *in vitro* study indicated that human lung adenocarcinoma cells were sensitive to batumin (Fig. 2). Therefore, we performed a pilot study of anticancer activity of batumin using Lewis

lung carcinoma in mice (3LL) as a model to study the effect of batumin *in vivo*. Batumin was administered by i.p. injections at a total dose of 3.15 mg per mouse divided in 9 equal i.p. injections (350 μg of batumin in 0.5 mL physiologic solution per mouse per injection). Primary tumor growth dynamics was monitored daily starting from day 7 after 3LL transplantation until the end of the experiment on day 23. In this experiment, we relied on earlier done assessment of batumin toxicity *in vivo*, and did not perform the toxicity study. Visually, the control and experimental animals presented no differences in behaviour and weight (data not shown).

Administration of batumin at metronomic regimen significantly reduced the number and total volume of metastases in mice. The number of lung metastases was reduced by two-fold in the batumin treated animals when compared to the control group resulting in a statistically significant difference with $P < 0.05$. The total volume of metastases was nearly 10 times lower in the batumin treated animals as compared to the control group ($P < 0.05$). However, 14% of the inhibitory effect of batumin on primary tumor growth was below the statistical reliability with $P > 0.05$ (Table 3). Thus, it was concluded that the administration of batumin at a metronomic regimen caused a significant anti-metastatic effect in 3LL-bearing animals.

Conclusion

Batumin has been used in the composition of an experimental 0.1% batumin ointment for the treatment and prevention of *S. aureus* nasal carriage at concentrations, which have been shown in this work to be therapeutic against melanoma cells [34]. No significant side effects of the ointment application have been reported. This work demonstrates an unexpected anti-cancer activity of batumin, which was known before as an antibiotic against *S. aureus*. This activity was predicted by *in silico* screening against the PharmaDB database of pharmacophores for possible binding sites of this antibiotic. Predicted affinity to the active centers of two cancer related proteins was confirmed by molecular docking modeling and in experimental trials conducted in two independent laboratories using different approaches of cytotoxicity trials.

Computational modeling suggests that batumin may induce apoptosis in several types of cancer cells by binding to the MDM2 active center of the p53 transcriptional regulator which prevents inhibition of this protein in cancer cells [26]. Cell cycle progression studies suggested that batumin may induce apoptosis since an increase in the percentage of cells occupying the phase

sub-G_1 was observed. This hypothesis was supported by light microscopic study of morphological changes in batumin treated cells. Induction of apoptosis by batumin has not been reported before. Although this effect was observed for both melanoma cells and normal skin keratinocytes, possible apoptosis induction by batumin was more prominent in the melanoma cells. This observation may explain the observed difference in the cytotoxicity of batumin on UCT-Mel 1 and HaCat cells (Fig. 1 and Table 2). Furthermore, it was demonstrated that the cell line specific toxicity of batumin had the highest activity against melanoma and lung carcinoma cells, with moderate to no toxicity against other tested cancer cells and normal skin keratinocytes. The potential of batumin as a possible anti-cancer drug was further supported by the results of the *in vivo* experiment on mice transplanted with 3LL cells. While the primary tumor remained basically unaffected, injections of batumin significantly reduced the number and total volume of metastases in experimental mice. Potential anticancer activity of polyene antibiotics and their ability to potentiate significantly the effect of other antibiotics has been reported previously. However, the extreme versatility of these natural compounds did not allow identification of any structural element correlated with observed antibacterial and/or anticancer activities [31]. Strongly specific cytotoxicity against several melanoma cell lines was reported for a polyene marinomycins synthesized by marine actinomycetes [32]. However, the structure of these circular macrodiolide antibiotics is not similar to the structure of batumin to be able to speculate about any commonality of the mechanisms of their cytotoxicity.

Future perspective

This study demonstrated culture specific toxicity of batumin against melanoma and lung carcinoma cells. Light microscopy and cell cycle progression results suggest the induction of apoptosis as a possible type of cell death. *In vitro* data obtained from this study warrants future research on assessing batumin's potential as antiproliferative agent and its involvement in the extrinsic- and extrinsic pathway of apoptosis by caspase dependent- or independent pathways to unravel its mechanism of action in cell death and the prospects of its application as an anticancer agent [33]. Additional studies to assess the potential anti-proliferative effect of batumin and prospects of its application as an anticancer agent should be conducted also. The most striking was the result that melanoma cells were 20 fold more sensitive to batumin than the normal keratinocytes. High toxicity of anti-cancer drugs is one of the major problems of chemotherapy.

Consider, for example, the cytotoxicity of actinomycin D in Table 2. It looks prospective to use batumin as a model to study culture specific mechanisms of cytotoxicity for future design of effective non-toxic anti-cancer drugs.

Executive summary

- Batumin was laboratory extracted for this study from the culture medium of *Pseudomonas batumici*.
- Batumin significantly inhibits the growth of UCT-Mel 1 melanoma and A549 human lung adenocarcinoma cell lines.
- Batumin showed low toxicity against HaCat skin keratinocytes that was 20 fold lower than that detected for melanoma cells.
- Injections of batumin significantly reduce the number and volume of metastases in 3LL Lewis lung carcinoma transplanted mice.
- Cell morphology, cell cycle progression studies and molecular docking modeling suggested the possibility of apoptosis induction in batumin-treated cancer cells.
- Reduced toxicity of batumin suggests possibility to use this antibiotic for melanoma prophylaxis.

Financial & competing interests disclosure

AMJ acquired grants from the National Research Foundation (NRF; 105992, 90523 and 85818), Cancer Association of South Africa (A0V741 and A0W228), the Struwig Germeshuysen Trust (A0N074), the School of Medicine Research Committee of the University of Pretoria and Medical Research Council (A0W110). MHV was funded from the NRF (99706), the School of Medicine Research Committee of the University of Pretoria and Struwig Germeshysen Trust (no grant numbers). NL was funds from NRF/IKS160514165042 Grant No: 105169. ONR was funded from NRF grant 95866.

The authors have no other relevant affiliations or financial involvement with any organization or entity with a financial interest in or financial conflict with the subject matter or materials discussed in the manuscript apart from those disclosed.

Acknowledgements

The authors want to acknowledge the continuing support to this research by the founder of batumin, Prof. Kiprianova EA (Kyiv, Ukraine). The authors thank Prof. Lester Davids from the Department of Human Biology at the University of Cape Town (RSA) for donating us UCT-Mel 1 and HaCat cell lines for this research. The authors also thank Dr. Rian Pierneef from the Center for Bioinformatics and Computational Biology in the Department of Biochemistry, Genetics and Microbiology at the University of Pretoria (RSA) for reviewing and correcting the manuscript.

References

1. Garattini S, Bertele V. Efficacy, safety, and cost of new anticancer drugs. *BMJ* 325, 269-271 (2002).
2. Calvert H, Jodrell DI, Cassidy J, Harris AL. Efficacy, safety, and cost of new anticancer drugs. Pessimistic conclusion was not justified. *BMJ* 325, 1302 (2002).
3. Cuzick J, Powles T, Veronesi U, Forbes J, Edwards R, Ashley S, Boyle P. Overview of the main outcomes in breast-cancer prevention trials. *Lancet*. 361, 296-300 (2003).
4. Vaishnav P, Demain AL. Unexpected application of secondary metabolites. *Biotechnol. Adv*. 29, 223-229 (2011).

****** **This article gives a comprehensive overview of activities of various secondary metabolites.**

5. Sliwoski G, Kothiwale S, Meiler J, Lowe EW Jr. Computational methods in drug discovery. *Pharmacol. Rev*. 66, 334-395 (2013).
6. Mattheus W, Gao LJ, Herdewijn P, Landuyt B, Verhaegen J, Masschelein J, Volckaert G, Lavigne R. Isolation and purification of a new kalimantacin/batumin-related polyketide antibiotic and elucidation of its biosynthesis gene cluster. *Chem. Biol*. 17, 149-159 (2010).

***** **This article gives an overview of kalimantacin/batumin-related antibiotics.**

7. Kiprianova EA, Klochko VV, Zelena LB, Churkina LN, Avdeeva LV. *Pseudomonas batumici* sp. nov., the antibiotic-producing bacteria isolated from soil of the Caucasus Black Sea coast. *Mikrobiol. Z.* 73, 3-8 (2011).
8. Mattheus W, Masschelein J, Gao LJ, Herdewijn P, Landuyt B, Volckaert G, Lavigne R. The kalimantacin/batumin biosynthesis operon encodes a self-resistance iso-form of the FabI bacterial target. *Chem. Biol*. 17, 1067-1071 (2010).

*** This article explains in detail the biosynthesis of kalimantacin/batumin-related antibiotics.**

9. Klochko VV, Zelena LB, Kim JY, Avdeeva LV, Reva ON. Prospects of a new antistaphylococcal drug batumin revealed by molecular docking and analysis of the complete genome sequence of the batumin-producer *Pseudomonas batumici* UCM B-321. *Int. J. Antimicrob. Agents*. 47, 56-61 (2016).

*** This article gives an additional information on molecular docking of batumin.**

10. Lee VE, O'Neill AJ. Batumin does not exert its antistaphylococcal effect through inhibition of aminoacyl-tRNA synthetase enzymes. *Int. J. Antimicrob. Agents*. 49, 121-122 (2017).
11. Hamilton-Miller JM. Chemistry and biology of the polyene macrolide antibiotics. *Bacteriol. Rev*. 37, 166-196 (1973).

**** This article gives an overview of mechanisms of action of various polyene antibiotics.**

12. Gomes ES, Schuch V, de Macedo Lemos EG. Biotechnology of polyketides: new breath of life for the novel antibiotic genetic pathways discovery through metagenomics. *Braz. J. Microbiol*. 44, 1007-1034 (2014).
13. Thistlethwaite IRG, Bull FM, Cui C, Walker PD, Gao SS, Wang L, Song Z, Masschelein J, Lavigne R, Crump MP, Race PR, Simpson TJ, Willis CL. Elucidation of the relative and absolute stereochemistry of the kalimantacin/batumin antibiotics. *Chem. Sci*. 8, 6196-6201 (2017).

*** This article elucidates properties and activities of kalimantacin/batumin-related antibiotics through their stereochemistry.**

14. Woerly EM, Roy J, Burke MD. Synthesis of most polyene natural product motifs using just 12 building blocks and one coupling reaction. *Nat. Chem*. 6, 484-491 (2014).
15. Klochko VV. Biosynthesis and properties of antibiotic batumin. *Biotechnologia Acta*; 7, 46-50 (2014).
16. Mosman T. Rapid colorimetric assay for cellular growth and survival: application to proliferation and cytotoxicity assays. *Immunol. Methods* 65, 55-63 (1983).
17. Zheng, Y.T., Chan, W.L., Chan, P., Huang, H. and Tam, S.C. Enhancement of the anti-herpetic effect of trichosanthin by acyclovir and interferon. *FEBS Letters* 496, 139-142 (2001).
18. Kirk JM. The mode of action of actinomycin D. *Biochimica et Biophysica Acta* 42, 167-169 (1960).
19. Kurpeshev OK, Osinsky SP, Florovskaya NY, Silantieva NK, Lebedeva TB. Lifespan of patients with metastatic colorectal cancer in the liver after incomplete courses of chemotherapy or symptomatic treatment. *Oncology (Ukraine)* 15: 301-306 (2013).
20. Lillie RD. Histopathologic technic and practical histochemistry. *McGaw-Hill Book Co*., New York, 445 (1965).
21. Riccardi C, Nicoletti I. Analysis of apoptosis by propidium iodide staining and flow cytometry. *Nat. Protoc*. 1, 1458-1461 (2006).
22. Meslamani J, Rognan D. Protein-Ligand Pharmacophores: Concept, Design and Applications. *CICSJ Bulletin*. 33, 27 (2015).
23. Diller DJ, Merz KM Jr. High throughput docking for library design and library prioritization. *Proteins* 43, 113-124 (2001).
24. Berman HM, Westbrook J, Feng Z, Gilliland G, Bhat TN, Weissig H, Shindyalov IN, Bourne PE. The protein data bank. *NAR* 28, 235-242 (2000).
25. Bézivin C, Tomasi S, Lohézic-Le Dévéhat F, Boustie J. Cytotoxic activity of some lichen extracts on murine and human cancer cell lines. *Phytomedicine* 10, 499-503 (2003).
26. Zhang Q, Zeng SX, Lu H. Targeting p53-MDM2-MDMX loop for cancer therapy. *Subcell. Biochem*. 85, 281-319 (2014).
27. Vaupel A, Bold G, De Pover A, Stachyra-Valat T, Lisztwan JH, Kallen J, Masuya K, Furet P. Tetra-substituted imidazoles as a new class of inhibitors of the p53-MDM2 interaction. *Bioorg. Med. Chem. Lett*. 24, 2110-2114 (2014).
28. Yu M, Wang Y, Zhu J, Bartberger MD, Canon J, Chen A, Chow D, Eksterowicz J, Fox B, Fu J, Gribble M, Huang X, Li Z, Liu JJ, Lo MC, McMinn D, Oliner JD, Osgood T, Rew Y, Saiki

AY, Shaffer P, Yan X, Ye Q, Yu D, Zhao X, Zhou J, Olson SH, Medina JC, Sun D. Discovery of potent and simplified piperidinone-based inhibitors of the MDM2-p53 interaction. *ACS Med. Chem. Lett*. 5, 894-899 (2014).

29. Addie M, Ballard P, Buttar D, Crafter C, Currie G, Davies BR, Debreczeni J, Dry H, Dudley P, Greenwood R, Johnson PD, Kettle JG, Lane C, Lamont G, Leach A, Luke RW, Morris J, Ogilvie D, Page K, Pass M, Pearson S, Ruston L. Discovery of 4-amino-N-[(1S)-1-(4-chlorophenyl)-3-hydroxypropyl]-1-(7H-pyrrolo[2,3-d]pyrimidin-4-yl) piperidine-4-carboxamide (AZD5363), an orally bioavailable, potent inhibitor of Akt kinases. *J. Med. Chem*. 56, 2059-2073 (2013).

30. Kroemer G, Galluzzi L, Vandenabeele P, Abrams J, Alnemri ES, Baehrecke EH, Blagosklonny MV, El-Deiry WS, Golstein P, Green DR, Hengartner M, Knight RA, Kumar S, Lipton SA, Malorni W, Nuñez G, Peter ME, Tschopp J, Yuan J, Piacentini M, Zhivotovsky B, Melino G; Nomenclature Committee on Cell Death 2009. Classification of cell death: recommendations of the Nomenclature Committee on Cell Death 2009. *Cell Death Differ*. 16, 3-11 (2009).

31. Valeriote F, Medoff G, Dieckman J. Potentiation of cytotoxicity of anticancer agents by several different polyene antibiotics. *J. Natl. Cancer Inst*. 72, 435-439 (1984).

32. Kwon HC, Kauffman CA, Jensen PR, Fenical W. Marinisporolides, polyene-polyol macrolides from a marine actinomicete of the new genus *Marinispora*. *J. Org. Chem*. 74, 675-684 (2009).

33. Zhang XD, Gillespie SK, Hersey P. Staurosporine induces apoptosis of melanoma by both caspase-dependent and -independent apoptotic pathways. *Mol. Cancer Ther*. 3, 187-197 (2004).

34. Churkina L, Kiprianova E, Bidnenko S, Marchenko K, Artysyuk E. Antibiotic batumin for diagnostics of staphylococci and treatment of *Staphylococcus aureus* nasal carriage. *Lik. Sprava* 1-2, 61-67 (2009).